Interaction measures for control configuration selection based on interval type-2 Takagi-Sugeno fuzzy model

Qian-Fang Liao, Da Sun

***Abstract*—Interaction measure determines decentralized and sparse control configurations for multivariable process control. This paper investigates interval type-2 Takagi-Sugeno fuzzy (IT2TSF) model based interaction measures using two different criteria, one is controllability and observability gramians, the other is relative normalized gain array (RNGA). The main contributions are i). A data-driven IT2TSF modeling method is introduced; ii). Explicit formulas to execute the two measures based on IT2TSF models are given; iii). Two interaction indexes are defined from RNGA to select sparse control configuration; iv). The calculations to derive sensitivities of the two measures with respect to parametric variations in the IT2TSF models are developed; v). The discussion to compare the two measures is presented. Three multivariable processes are used as examples to show that the results calculated from IT2TSF models are more accurate than that from their type-1 counterparts, and compared to gramian-based measure, RNGA selects more reasonable control configurations and is more robust to the parametric uncertainties.**

***Index Terms*—Interaction measure, control configuration, gramians, RNGA, type-2 fuzzy model.**

I. Introduction

Interaction measure is used to select a control configuration for multi-input-multi-output (MIMO) process control that determines which of the available process inputs should be used to regulate each of the outputs. A proper control configuration can greatly reduce the burden on control system to handle the interactions. For the popular decentralized control using simplest configuration where only one input is regulating one output, interaction measure can pair inputs and outputs 1-for-1 with minimum coupling effects among the paired input-output channels to relieve the controller of interactions suppressing. When no decentralized control yields a satisfactory performance due to the limited flexibility of 1-for-1 control configuration, interaction measure can choose several unpaired elements with relatively large dominance and add them to the pairing structure to determine a sparse control configuration.

Currently, a number of interaction measures are available and can be divided into two broad categories. One is composed of the methods [1]-[6] using controllability and observability gramians, the other is the group led by relative gain array (RGA) [7]. The gramian-based methods assess the interactions by combining the controllability and the observability of each channel. This study was originally proposed in [1] and further discussed in [2] to determine control configuration for linear MIMO processes. In [3] and [4], it was extended to bilinear and nonlinear processes. The Hankel interaction index array (HIIA) proposed in [5]-[6] is a similar study and can be included into this category. For the other category, RGA is actually a pioneer for interaction measure and much more widely applied than gramians. It is generally used in conjunction with Niederlinski index (NI) [8] to ensure the stability. RGA and NI are simple to apply because only steady-state gains of the channels are used. However, this fact may cause incorrect results since no dynamic information is included. [9] presents a comparison between RGA and HIIA to give a conclusion that both of them can select reasonable decentralized control configurations, but HIIA offers a deeper insight into the interactions. Recently, several studies considering both steady and dynamic properties were proposed to enrich the RGA category. Such as the dynamic RGA methods [10]-[12] using transfer functions in lieu of steady-state gains to compute RGA, the effective relative gain array [13] including bandwidth for interaction measure, and the relative normalized gain array (RNGA) [14] choosing response speed together with RGA and NI to select control configuration. Among them, RNGA gives a comprehensive description of dynamic interactions without requiring specifics of controllers, and offers reasonable results regardless of the process's dimension, and its computational cost is acceptable. [3]-[4] states that gramian-based methods are superior to RGA family since gramians can quantify the relative dominance of the unpaired channels for sparse control configuration selection while RGA cannot. The study in [15] uses RNGA to determine sparse control configurations, which defends the RGA family.

Most of the studies concerning interaction measures are developed based on knowing the exact mathematical functions of the process, and the major part of them are using linear transfer functions. In the real applications, exact mathematical process functions are generally difficult to obtain, and the linear transfer function is insufficient to describe the nonlinear and complex processes. In addition, the studies of gramians based on bilinear and nonlinear functions in [3]-[4] determine only one decentralized or sparse control configuration for the whole working range which ignore the fact that different working conditions may require different control configurations. [16]-[17] investigated fuzzy-model-based interaction analyses using RGA and RNGA respectively to provide a solution for the aforementioned problems because **i)**. fuzzy models can be identified to a high degree of accuracy using data samples and

human experience thus no mathematical functions are required [18]; **ii)**. The control configurations are determined by taking working condition into account. To the best of author's knowledge, no work has been presented to implement gramian-based interaction measures based on fuzzy models.

This paper investigates the two interaction measures, gramians and RNGA, based on interval type-2 Takagi-Sugeno fuzzy (IT2TSF) models [19]. The main contributions are: **i)**. A data-driven method to construct IT2TSF models for the MIMO processes is introduced; **ii)**. Explicit formulas are developed to execute the two measures based on IT2TSF models; **iii)**. Two interaction indexes defined from RNGA are proposed to give a safer and more reasonable criterion to select sparse control configuration than that in [15]; **iv)**. The calculations to derive the sensitivities of the two measures with respect to parametric variations in the IT2TSF models are presented; **v)**. The discussion to analyze and compare the two measures is given. Three MIMO processes are used as examples to demonstrate that the proposed IT2TSF modeling method achieves higher accuracy than its type-1 counterpart, and compared to gramians, RNGA selects more reasonable control configurations and is more robust to the parametric uncertainties.

II. Interval type-2 T-S fuzzy modeling for MIMO processes

The traditional type-1 T-S fuzzy model can be expressed by:

Rule l ($l = 1, \cdots, L$): if $x(k)$ is Z^l, then
$$y^l(k) = a_1^l x_1(k) + a_2^l x_2(k) \cdots + a_p^l x_p(k) \quad (1)$$

where L is the number of fuzzy rules; $x(k) = [x_1(k) \ \cdots \ x_p(k)]^T \in R^p$ is the input vector composed of premise variables; Z^l is a fuzzy set where the fuzzy membership for $x(k)$ is denoted by $\mu^l(x(k)) \in [0,1]$, $\sum_{l=1}^{L} \mu^l(x(k)) = 1$; a_r^l 's ($r = 1, \cdots, p$) are local model's coefficients; $y^l(k)$ is the local output. The total output is:

$$y(k) = \frac{\sum_{l=1}^{L} \mu^l(x(k)) y^l(k)}{\sum_{l=1}^{L} \mu^l(x(k))} = \sum_{l=1}^{L} \mu^l(x(k)) y^l(k) \quad (2)$$

Compared to the type-1 T-S fuzzy model, IT2TSF model is using intervals instead of crisp numbers to characterize fuzzy membership grades and local model's coefficients, which endows it additional design degree and makes it possible to directly describe the situations with inexactness [19]-[21]. An IT2TSF model consists of the following fuzzy rules:

Rule l ($l = 1, \cdots, L$): if $x(k)$ is $\tilde{Z}^l$, then
$$\tilde{y}^l(k) = \tilde{a}_1^l x_1(k) + \tilde{a}_2^l x_2(k) \cdots + \tilde{a}_p^l x_p(k) \quad (3)$$

where $\tilde{Z}^l$ is an interval type-2 fuzzy set where the fuzzy membership for $x(k)$ is an interval denoted by $\tilde{\mu}^l(x(k)) = [\underline{\mu}^l(x(k)), \ \overline{\mu}^l(x(k))]$, $\underline{\mu}(x(k))$ and $\overline{\mu}(x(k))$ are lower and upper bounds respectively satisfying $0 \le \underline{\mu}(x(k)) \le \overline{\mu}(x(k)) \le 1$. The local model's coefficients are intervals: $\tilde{a}_r^l = [\underline{a}_r^l, \ \overline{a}_r^l]$ ($r = 1, \cdots, p$), subsequently, the local outputs are also intervals $\tilde{y}^l(k) = [\underline{y}^l(k), \ \overline{y}^l(k)]$ and derived by:

$$\begin{cases} \underline{y}^l(k) = \underline{a}_1^l x_1(k) + \underline{a}_2^l x_2(k) \cdots + \underline{a}_p^l x_p(k) \\ \overline{y}^l(k) = \overline{a}_1^l x_1(k) + \overline{a}_2^l x_2(k) \cdots + \overline{a}_p^l x_p(k) \end{cases} \quad (4)$$

Blending the L local outputs $\tilde{y}^l(k)$ by the fuzzy membership functions $\tilde{\mu}^l(x(k))$ can give a type-reduced set [19], which is an interval denoted as $\tilde{y}(k) = [\underline{y}(k), \ \overline{y}(k)]$. Afterwards, the crisp output $y(k)$ can be derived by defuzzifying $\tilde{y}(k)$. A number of type-reduction and defuzzification methods [19]-[23] are available for IT2TSF system. Such as the popular Karnik-Mendel algorithms [19]-[21], which require iterative calculation. In this paper, we choose the following simple type-reduction method [22]-[23] to save the iterative calculation:

$$\begin{cases} \underline{y}(k) = \sum_{l=1}^{L} \underline{\mu}^l(x(k)) \underline{y}^l(k) / \sum_{l=1}^{L} \underline{\mu}^l(x(k)) \\ \overline{y}(k) = \sum_{l=1}^{L} \overline{\mu}^l(x(k)) \overline{y}^l(k) / \sum_{l=1}^{L} \overline{\mu}^l(x(k)) \end{cases} \quad (5)$$

Subsequently, the centroid defuzzification is used to derive the crisp total output of the IT2TSF model:

$$y(k) = (\underline{y}(k) + \overline{y}(k))/2 \quad (6)$$

This paper proposes a data-driven method to identify fuzzy models. Firstly, a type-1 T-S fuzzy model is built. Afterwards, the crisp coefficients of the type-1 fuzzy model are extended to intervals to achieve an IT2TSF model. The steps are as follows:

i). Collect N input-output samples from the original process as: $z(k) = [x^T(k) \ \ y(k)]^T$, $k = 1, \cdots, N$, and choose a proper number of fuzzy sets/fuzzy rules as L.

ii). Use Gustafson-Kessel clustering algorithm [24] to locate a center, denoted by $zc^l = [(xc^l)^T \ \ yc^l]^T$ ($l = 1, \cdots, L$) for each fuzzy set, and subsequently obtain a crisp fuzzy membership matrix for all data denoted by $\mathcal{U} = [\mu^l(z(k))]_{L \times N}$, where $0 \le \mu^l(z(k)) \le 1$ and $\sum_{l=1}^{L} \mu^l(z(k)) = 1$.

iii). Use weighted least square method to identify the crisp local models' coefficients:

$$P^l = (X^T M^l X)^{-1} X^T M^l Y, \ l = 1, \cdots, L \quad (7)$$

where $P^l = [a_1^l \ \cdots \ a_p^l]^T \in R^p$, $M^l = diag\{\mu^l(z(1)), \ \cdots, \ \mu^l(z(N))\} \in R^{N \times N}$ are weight matrix, $X = [x(1) \ \cdots \ x(N)]^T \in R^{N \times p}$, and $Y = [y(1) \ \cdots \ y(N)]^T \in R^N$.

Steps **i)-iii)** build a type-1 T-S fuzzy model. Taking it as a base, an IT2TSF model can be obtained by extending the fuzzy memberships $\mu^l(z(k))$ and local model's coefficients a_r^l to intervals using the varying radiuses $\Delta\mu^l \in [0,1]$ and Δa_r^l as:

$$\begin{cases} \underline{\mu}^l(z(k)) = \max[0, \quad \mu^l(z(k)) - \Delta\mu^l(1 - \mu^l(z(k)))] \\ \overline{\mu}(z(k)) = \min\left[1, \quad \mu^l\left(z(k)\right) + \Delta\mu^l(1 - \mu^l(z(k)))\right] \end{cases} \quad (8)$$

$$\underline{a}_r^l = a_r^l - \Delta a_r^l, \ \overline{a}_r^l = a_r^l + \Delta a_r^l \quad (9)$$

Choosing proper initial values $\Delta\mu^l(0)$ and $\Delta a_r^l(0)$, such as $\Delta\mu^l(0) = 0.1$ and $\Delta a_r^l(0) = 0$, the following steps introduce a learning process to obtain $\Delta\mu^l$ and Δa_r^l:

iv). Use Kalman filter algorithm to derive Δa_r^l as:

$$\begin{cases} \Delta P(k+1) = \Delta P(k) + S(k+1)\chi(k)[y(k) - y_{TS}(k)] \\ S(k+1) = \frac{1}{\xi}\left(S(k) - \frac{S(k)\chi(k)\chi^T(k)S(k)}{\xi + \chi^T(k)S(k)\chi(k)}\right) \end{cases} \quad (10)$$

where ΔP is a vector consisting of all radiuses of the local model's coefficients as $\Delta P = [\Delta a_1^1 \cdots \Delta a_p^1 \cdots \Delta a_1^L \cdots \Delta a_p^L]^T \in R^{pL}$; $\chi(k) = [h^1(k)x^T(k) \ \cdots \ h^L(k)x^T(k)]^T \in R^{pL}$, $h^l(k) = \frac{0.5\overline{\mu}^l(x(k))}{\sum_{l=1}^L \overline{\mu}^l(x(k))} - \frac{0.5\underline{\mu}^l(x(k))}{\sum_{l=1}^L \underline{\mu}^l(x(k))}$, $l = 1, \cdots, L$; $y(k)$ is the sampled output, and $y_{TS}(k)$ is IT2TSF model's output calculated by (6); $S(0) = S_0 I_{pL\times pL}$, S_0 is set as a large positive constant, such as $S_0 = 1000$; $I_{pL\times pL}$ is a $pL \times pL$ identity matrix; $\xi \in (0,1]$ is the forgetting factor, for example it can be set as $\xi = 0.9995$;

v). Use gradient descent learning to derive $\Delta\mu^l$:

$$\Delta\mu^l(k+1) = \Delta\mu^l(k) - \eta_\mu \frac{\partial E_y(k)}{\partial \Delta\mu^l(k)}, k = 0,1,\cdots,N \quad (11)$$

where η_μ is the learning step size, for example, $\eta_\mu = 0.1$; $E_y(k) = (y(k) - y_{TS}(k))^2/2$; $\partial E_y(k)/\partial\Delta\mu^l(k)$ is obtained according to [25]. The learning results are $\Delta\mu^l = \Delta\mu^l(N)$ and $\Delta a_r^l = \Delta a_r^l(N)$. The IT2TSF model identification is complete.

Remark 2.1: For the proposed IT2TSF modeling method, the persistent excitation of inputs can improve the identification accuracy, but it is not a necessary condition. In [26], an analysis is given to prove that using the recursive algorithm in (10) without persistent excitation hypothesis, the projection of the parametric error on the so-called "excitation subspace" tends to zero, while the orthogonal component of the error keeps bounded.

Remark 2.2: Noted that the coefficients Δa_r^l ($l = 1, \cdots, L$, $r = 1, \cdots, p$) determined by the proposed learning algorithms may be negative numbers, which means, it is possible that for some of the local model's coefficients $\tilde{a}_r^l = [\underline{a}_r^l, \ \overline{a}_r^l]$ to have $\underline{a}_r^l > \overline{a}_r^l$. In this case, we still let and denote the larger number as $\underline{a}_r^l$ and smaller one as $\overline{a}_r^l$ for convenience.

When giving a new input vector $x(k)$ to the IT2TSF model, firstly its L crisp fuzzy memberships are calculated by:

$$\mu^l(x(k)) = \begin{cases} 0, & \forall_{\substack{v=1,\ldots,L \\ v\neq l}} \|x(k) - xc^v\| = 0 \\ 1, & \|x(k) - xc^l\| = 0 \\ \frac{1}{\sum_{v=1}^L \frac{\|x(k)-xc^l\|}{\|x(k)-xc^v\|}}, & else \end{cases} \quad (12)$$

where $\|x(k) - xc^v\| = (x(k) - xc^v)^T(x(k) - xc^v)$. Afterwards, the upper and lower bounds of $\tilde{\mu}^l(x(k))$ can be derived using (8) replacing $z(k)$ by $x(k)$. The local and total outputs can be obtained through (4) and (6) respectively.

Assumption 2.1: The MIMO processes considered in this paper are open-loop stable, non-singular in steady-state conditions, and have equal number of inputs and outputs.

The following IT2TSF model matrix can describe an $n \times n$ process with n inputs u_j and n outputs y_i, $i, j = 1, \cdots, n$:

$$F_{TS} = [f_{TS,ij}]_{n\times n} = \begin{bmatrix} f_{TS,11} & \cdots & f_{TS,1n} \\ \vdots & \vdots & \vdots \\ f_{TS,n1} & \cdots & f_{TS,nn} \end{bmatrix} \quad (13)$$

where $f_{TS,ij}$ denotes the open-loop IT2TSF model for individual channel $y_i - u_j$, it has the following rules:

Rule l ($l = 1, \cdots, L_{ij}$): if $x_{ij}(k)$ is $\tilde{Z}_{ij}^l$, then

$$\tilde{y}_i^l(k) = \tilde{a}_{ij,1}^l y_i(k-1) + \cdots + \tilde{a}_{ij,p}^l y_i(k-p) + \tilde{b}_{ij,0}^l u_j(k-\tau_{ij}) + \tilde{b}_{ij,1}^l u_j(k-\tau_{ij}-1) + \cdots + \tilde{b}_{ij,q}^l u_j(k-\tau_{ij}-q) \quad (14)$$

where $x_{ij}(k) = [y_i(k-1)\cdots y_i(k-p) \ u_j(k-\tau_{ij})\cdots u_j(k-\tau_{ij}-q)]^T \in R^{p+q+1}$, $p \geq 1$ and $q \geq 0$ are integers, $\tau_{ij} = \tau'_{ij}/T$, τ'_{ij} is the time delay of $y_i - u_j$, and T is sampling time; The fuzzy membership of $x_{ij}(k)$ in $\tilde{Z}_{ij}^l$ is $\tilde{\mu}_{ij}^l(x_{ij}(k)) = [\underline{\mu}_{ij}^l(x_{ij}(k)), \ \overline{\mu}_{ij}^l(x_{ij}(k))]$; $\tilde{a}_{ij,r}^l = [\underline{a}_{ij,r}^l, \ \overline{a}_{ij,r}^l]$ ($r = 1, \cdots, p$) and $\tilde{b}_{ij,s}^l = [\underline{b}_{ij,s}^l, \ \overline{b}_{ij,s}^l]$ ($s = 0,1,\cdots,q$) are local model's coefficients. The data samples $z_{ij}(k) = [x_{ij}^T(k) \ y_i(k)]^T$, $k = 1, \cdots, N$, of the open-loop $y_i - u_j$ are always obtainable through appropriate excitations [27] for model identification. F_{TS} is the base to derive steady and dynamic information of the MIMO process for interaction measure.

III. Interaction Measures for Control Configuration Selection

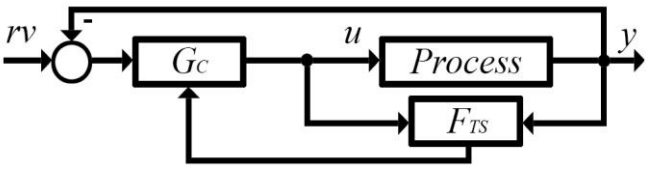

Fig. 1. A fuzzy-model-based closed-loop control system

A general fuzzy-model-based control system is shown in Fig. 1, where $rv = [rv_1 \ \cdots \ rv_n]^T$ are reference values, $G_c = [g_{c,ij}]_{n\times n}$ is the MIMO controller. The interaction measure selects dominant channels from F_{TS} to from a nominal model, denoted by $\overline{F}_{TS}$, to subsequently determine a configuration for G_c, whose structure is the transpose of that of $\overline{F}_{TS}$ [15],[28]. For example, a 3×3 process F_{TS} where inputs and outputs are paired 1-for-1 have three dominant channels as: $y_1 - u_2/y_2 - u_3/y_3 - u_1$, then $\overline{F}_{TS}$ and decentralized controller G_c are:

$$\overline{F}_{TS} = \begin{bmatrix} 0 & f_{TS,12} & 0 \\ 0 & 0 & f_{TS,23} \\ f_{TS,31} & 0 & 0 \end{bmatrix} \rightarrow G_c = \begin{bmatrix} 0 & 0 & g_{c,13} \\ g_{c,21} & 0 & 0 \\ 0 & g_{c,32} & 0 \end{bmatrix}$$

When the 1-for-1 structure cannot fully handle the channel interactions, we can increase the configuration complexity by adding the unpaired element(s) with relatively large dominance to $\overline{F}_{TS}$ to give a sparse control configuration for G_c. Suppose $y_1 - u_1$ and $y_3 - u_2$ in the above example are selected, then:

$$\overline{F}_{TS} = \begin{bmatrix} f_{TS,11} & f_{TS,12} & 0 \\ 0 & 0 & f_{TS,23} \\ f_{TS,31} & f_{TS,32} & 0 \end{bmatrix} \rightarrow G_c = \begin{bmatrix} g_{c,11} & 0 & g_{c,13} \\ g_{c,21} & 0 & g_{c,23} \\ 0 & g_{c,32} & 0 \end{bmatrix}$$

Due to the nonlinear nature of fuzzy model, an operating point should be given to calculate the steady and dynamic information to proceed with the interaction measure as well as to adapt different working conditions. For $f_{TS,ij}$, given an operating point as:

$$x_{ij}(k_0) = [y_i(k_0-1)\cdots y_i(k_0-p)\ \ u_j(k_0-\tau_{ij})\cdots u_j(k_0-\tau_{ij}-q)]^T \quad (15)$$

In the working condition around $x_{ij}(k_0)$, $f_{TS,ij}$ can be represented using the following linear functions by setting $\mu_{ij}^l(x_{ij}(k)) = \mu_{ij}^l(x_{ij}(k_0))$ [17]:

$$y_i(k) = a_{ij,1}y_i(k-1) + \cdots + a_{ij,p}y_i(k-p) + b_{ij,0}u_j(k-\tau_{ij}) + \cdots + b_{ij,q}u_j(k-\tau_{ij}-q) \quad (16)$$

where $a_{ij,r}$ $(r = 1,\cdots,p)$ and $b_{ij,s}$ $(s = 0,1,\cdots,q)$ are

$$a_{ij,r} = \frac{1}{2}\left(\frac{\sum_{l=1}^{L_{ij}}\underline{\mu}_{ij}^l(x_{ij}(k_0))\underline{a}_{ij,r}^l}{\sum_{l=1}^{L_{ij}}\underline{\mu}_{ij}^l(x_{ij}(k_0))} + \frac{\sum_{l=1}^{L_{ij}}\overline{\mu}_{ij}^l(x_{ij}(k_0))\overline{a}_{ij,r}^l}{\sum_{l=1}^{L_{ij}}\overline{\mu}_{ij}^l(x_{ij}(k_0))}\right) \quad (17)$$

$$b_{ij,s} = \frac{1}{2}\left(\frac{\sum_{l=1}^{L_{ij}}\underline{\mu}_{ij}^l(x_{ij}(k_0))\underline{b}_{ij,s}^l}{\sum_{l=1}^{L_{ij}}\underline{\mu}_{ij}^l(x_{ij}(k_0))} + \frac{\sum_{l=1}^{L_{ij}}\overline{\mu}_{ij}^l(x_{ij}(k_0))\overline{b}_{ij,s}^l}{\sum_{l=1}^{L_{ij}}\overline{\mu}_{ij}^l(x_{ij}(k_0))}\right) \quad (18)$$

Equation (16) can be expressed in the state-space form:

$$X_{ij}(k+1) = A_{0,ij}X_{ij}(k) + B_{0,ij}U_{ij}(k-\tau_{ij})$$
$$y_i(k) = C_{0,ij}X_{ij}(k) \quad (19)$$

where $X_{ij}(k) = [y_i(k-p+1)\ \ \cdots\ \ y_i(k-1)\ \ y_i(k)]^T$, $U_{ij}(k-\tau_{ij}) = [u_j(k-\tau_{ij}-q+1)\ \ \cdots\ \ u_j(k-\tau_{ij}+1)]^T$,

$$A_{0,ij} = \begin{bmatrix} 0 & 1 & 0 & \cdots & 0 \\ 0 & 0 & 1 & \cdots & 0 \\ \vdots & \vdots & \vdots & \ddots & \vdots \\ 0 & 0 & 0 & \cdots & 1 \\ a_{ij,p} & a_{ij,p-1} & a_{ij,p-2} & \cdots & a_{ij,1} \end{bmatrix} \in R^{p\times p}, \quad B_{0,ij} = \begin{bmatrix} 0 & \cdots & 0 \\ \vdots & \vdots & \vdots \\ 0 & \cdots & 0 \\ b_{ij,q} & \cdots & b_{ij,0} \end{bmatrix} \in R^{p\times(q+1)}, \quad C_{0,ij} = [0\ \ \cdots\ \ 0\ \ 1] \in R^{1\times p}.$$

A. Gramian-based interaction measure

For $y_i - u_j$, equation (19) can be used to calculate a controllability gramian, $W_{ct,ij} \in R^{p\times p}$, and an observability gramian, $W_{ob,ij} \in R^{p\times p}$, which are symmetric and non-negative definite matrices depending on the state-space realization. The trace of their product, denoted by $tr_{ij} = trace\{W_{ct,ij}W_{ob,ij}\}$, is non-negative and realization independent, and demonstrates a combination of controllability and observability which characterizes the degree of dominance for u_j to y_i. Thus, it can be used as an interaction measure [2].

When $\tau_{ij} = 0$ in (19), $W_{ct,ij}$ and $W_{ob,ij}$ satisfy the following Lyapunov equations [2]:

$$A_{0,ij}W_{ct,ij}A_{0,ij}^T - W_{ct,ij} + B_{0,ij}B_{0,ij}^T = 0 \quad (20)$$
$$A_{0,ij}^T W_{ob,ij}A_{0,ij} - W_{ob,ij} + C_{0,ij}^T C_{0,ij} = 0 \quad (21)$$

which can be solved by (22) and (23) to obtain tr_{ij}:

$$W_{ct,ij} = \sum_{v=0}^{\infty}(A_{0,ij})^v B_{0,ij}B_{0,ij}^T(A_{0,ij}^T)^v \quad (22)$$
$$W_{ob,ij} = \sum_{v=0}^{\infty}(A_{0,ij}^T)^v C_{0,ij}^T C_{0,ij}(A_{0,ij})^v \quad (23)$$

Denote the controllability and observability gramians and the trace of their product when $\tau_{ij} = 0$ as $W_{ct,ij}^{(0)}$, $W_{ob,ij}^{(0)}$ and $tr_{ij}^{(0)}$ respectively. When $\tau_{ij} > 0$ in (19), tr_{ij} is derived by [2]:

$$tr_{ij} = tr_{ij}^{(0)} + \tau_{ij}C_{0,ij}W_{ct,ij}^{(0)}C_{0,ij}^T \quad (24)$$

Note that $C_{0,ij}W_{ct,ij}^{(0)}C_{0,ij}^T$ in (24) is equal to the element of $W_{ct,ij}^{(0)}$ in row p and column p for (19).

For the overall $n \times n$ process, we have $TR = [tr_{ij}]_{n\times n}$, and a participation matrix (PM) can be defined as [1]-[4]:

$$PM = [\psi_{ij}]_{n\times n} = \left[\frac{tr_{ij}}{\sum_{i=1}^n\sum_{j=1}^n tr_{ij}}\right]_{n\times n} \quad (25)$$

which implies $0 \le \psi_{ij} \le 1$ and $\sum_{i=1}^n\sum_{j=1}^n\psi_{ij} = 1$. ψ_{ij} quantifies the significance of $y_i - u_j$ that a larger/smaller ψ_{ij} means $f_{TS,ij}$ has the states easier/harder to control or observe and $y_i - u_j$ should be/not be a dominant channel. Therefore, the rules to determine $\overline{F}_{TS}$ based on PM are [2]:

i). *The paired elements achieve the maximum sum of ψ_{ij}'s*;

ii). *The paired and unpaired channels in $\overline{F}_{TS}$ achieve $\sum\psi_{ij} \ge 0.7$ with minimum number of nonzero elements.*

Remark 3.1: When using PM to select input-output pairs for decentralized control, in order to achieve the maximum $\sum\psi_{ij}$, the channel with largest ψ_{ij} may not be included into $\overline{F}_{TS}$.

Note that (22) and (23) contain the calculation of the sum of a geometric sequence $(A_{0,ij})^v$. Explicit formulas are needed to derive tr_{ij}. We choose two cases of $f_{TS,ij}$, which are equivalent to first order and second order functions that are widely used in applications, to investigate the explicit formulas:

Case 1: $p = 1$ and $q = 0$; **Case 2**: $p = 2$ and $q = 0$.

Theorem 3.1: For Case 1, tr_{ij} can be derived by:

$$tr_{ij} = b_{ij,0}^2\frac{1}{(1-a_{ij,1}^2)^2} + \frac{\tau_{ij}\times b_{ij,0}^2}{1-a_{ij,1}^2} \quad (26)$$

For Case 2, the formula to obtain tr_{ij} is

$$tr_{ij} = b_{ij,0}^2\frac{(1-a_{ij,2})^2(1+a_{ij,2}^2)+2a_{ij,1}^2a_{ij,2}}{[(1-a_{ij,2})^2-a_{ij,1}^2]^2(1+a_{ij,2})^2} + \frac{\tau_{ij}\times b_{ij,0}^2\times(1-a_{ij,2})}{[(1-a_{ij,2})^2-a_{ij,1}^2](1+a_{ij,2})} \quad (27)$$

Proof: For Case 1, the coefficients in (19) are: $A_{0,ij} = a_{ij,1}$, $B_{0,ij} = b_{ij,0}$ and $C_{0,ij} = 1$, according to Assumption 2.1, $|a_{ij,1}| < 1$. Then (22) and (23) can be rewritten by

$$W_{ct,ij} = \sum_{v=0}^{\infty}(a_{ij,1})^{2v}b_{ij,0}^2 = b_{ij,0}^2/(1-a_{ij,1}^2) \quad (28)$$
$$W_{ob,ij} = \sum_{v=0}^{\infty}(a_{ij,1})^{2v} = 1/(1-a_{ij,1}^2) \quad (29)$$

Submitting (28) and (29) to (24) can have (26).

For Case 2, $A_{0,ij} = \begin{bmatrix} 0 & 1 \\ a_{ij,2} & a_{ij,1} \end{bmatrix}$, $B_{0,ij} = \begin{bmatrix} 0 \\ b_{ij,0} \end{bmatrix}$ and $C_{0,ij} = [0\ \ 1]$. Denote the two eigenvalues of $A_{0,ij}$ as ρ_1 and ρ_2, according to Assumption 2.1, $|\rho_1| < 1$ and $|\rho_2| < 1$. If $A_{0,ij}$ is diagonalizable, $(A_{0,ij})^v$ can be calculated using Eigen decomposition:

$$(A_{0,ij})^v = \begin{bmatrix} 1 & 1 \\ \rho_1 & \rho_2 \end{bmatrix}\begin{bmatrix} \rho_1^v & 0 \\ 0 & \rho_2^v \end{bmatrix}\begin{bmatrix} 1 & 1 \\ \rho_1 & \rho_2 \end{bmatrix}^{-1} = \frac{1}{-\rho_1+\rho_2}\begin{bmatrix} \rho_1^v\rho_2 - \rho_1\rho_2^v & -\rho_1^v + \rho_2^v \\ \rho_1^{v+1}\rho_2 - \rho_1\rho_2^{v+1} & -\rho_1^{v+1} + \rho_2^{v+1} \end{bmatrix} \quad (30)$$

Using (30), equations (22) and (23) become:

$$W_{ct,ij} = \frac{\sum_{v=0}^{\infty}\begin{bmatrix} (-\rho_1^v+\rho_2^v)^2 & * \\ (-\rho_1^v+\rho_2^v)(-\rho_1^{v+1}+\rho_2^{v+1}) & (-\rho_1^{v+1}+\rho_2^{v+1})^2 \end{bmatrix}}{(-\rho_1+\rho_2)^2/b_{ij,0}^2}$$
$$= \frac{\begin{bmatrix} \frac{1}{1-\rho_1^2}-\frac{2}{1-\rho_1\rho_2}+\frac{1}{1-\rho_2^2} & * \\ \frac{\rho_1}{1-\rho_1^2}-\frac{\rho_1+\rho_2}{1-\rho_1\rho_2}+\frac{\rho_2}{1-\rho_2^2} & \frac{\rho_1^2}{1-\rho_1^2}-\frac{2\rho_1\rho_2}{1-\rho_1\rho_2}+\frac{\rho_2^2}{1-\rho_2^2} \end{bmatrix}}{(-\rho_1+\rho_2)^2/b_{ij,0}^2} \quad (31)$$

$$W_{ob,ij} = \frac{\sum_{v=0}^{\infty}\begin{bmatrix} (\rho_1^{v+1}\rho_2-\rho_1\rho_2^{v+1})^2 & * \\ (-\rho_1^{v+1}+\rho_2^{v+1})(\rho_1^{v+1}\rho_2-\rho_1\rho_2^{v+1}) & (-\rho_1^{v+1}+\rho_2^{v+1})^2 \end{bmatrix}}{(-\rho_1+\rho_2)^2}$$
$$= \frac{\begin{bmatrix} \frac{\rho_1^2\rho_2^2}{1-\rho_1^2}-\frac{2\rho_1^2\rho_2^2}{1-\rho_1\rho_2}+\frac{\rho_1^2\rho_2^2}{1-\rho_2^2} & * \\ -\frac{\rho_1^2\rho_2}{1-\rho_1^2}+\frac{\rho_1^2\rho_2+\rho_1\rho_2^2}{1-\rho_1\rho_2}-\frac{\rho_1\rho_2^2}{1-\rho_2^2} & \frac{\rho_1^2}{1-\rho_1^2}-\frac{2\rho_1\rho_2}{1-\rho_1\rho_2}+\frac{\rho_2^2}{1-\rho_2^2} \end{bmatrix}}{(-\rho_1+\rho_2)^2} \quad (32)$$

where $*$ denotes an element in symmetric matrix. Note that $A_{0,ij}$ has $\rho_1\rho_2 = -a_{ij,2}$ and $\rho_1 + \rho_2 = a_{ij,1}$. Submitting (31) and (32) to (24), after arrangement, we can have (27).

If $A_{0,ij}$ is not diagonalizable, in this case, $\rho_1 = \rho_2 = \rho$, $(A_{0,ij})^v$ can be calculated using Jordan matrix decomposition:

$$(A_{0,ij})^v = \begin{bmatrix} 1 & -1/\rho \\ \rho & 0 \end{bmatrix}\begin{bmatrix} \rho^v & v\rho^{v-1} \\ 0 & \rho^v \end{bmatrix}\begin{bmatrix} 1 & -1/\rho \\ \rho & 0 \end{bmatrix}^{-1}$$
$$= \begin{bmatrix} \rho^v(1-v) & v\rho^{v-1} \\ -v\rho^{v+1} & \rho^v(1+v) \end{bmatrix} \quad (33)$$

Submitting (33) into (22) and (23) can obtain:

$$W_{ct,ij} = \frac{b_{ij,0}^2}{(1-\rho^2)^3}\begin{bmatrix} 1+\rho^2 & * \\ 2\rho & 1+\rho^2 \end{bmatrix} \quad (34)$$

$$W_{ob,ij} = \frac{1}{(1-\rho^2)^3}\begin{bmatrix} (1+\rho^2)\rho^4 & * \\ -2\rho^3 & 1+\rho^2 \end{bmatrix} \quad (35)$$

Note that in this case, $A_{0,ij}$ has $a_{ij,1} = 2\rho$ and $a_{ij,2} = -\rho^2$, substituting (34) and (35) into (24), it is easy to find that the tr_{ij} in this case can still be calculated using (27).

B. RNGA based interaction measure

Two factors can be derived from (16) to proceed with the RNGA based interaction measure, one is steady-state gain, denoted by k_{ij}, the other is normalized integrated error, denoted by e_{ij}, which stands for the dynamic property of $f_{TS,ij}$ since larger/smaller e_{ij} implies slower/fast response speed [14],[17]:

$$k_{ij} = \frac{b_{ij,0}+b_{ij,1}+\cdots+b_{ij,q}}{1-(a_{ij,1}+a_{ij,2}+\cdots+a_{ij,p})} \quad (36)$$

$$e_{ij} = \frac{\sum_{v=0}^{q} v\cdot b_{ij,v} - \sum_{r=1}^{p}\sum_{s=0}^{q} a_{ij,r}\cdot b_{ij,s}\cdot|s-r|\cdot\mathrm{sgn}(s-r)}{(1-(a_{ij,1}+\cdots+a_{ij,p}))(b_{ij,0}+\cdots+b_{ij,q})}\cdot T + \tau_{ij}T \quad (37)$$

For the overall system, we have two matrices as $K = [k_{ij}]_{n\times n}$ and $E = [e_{ij}]_{n\times n}$ respectively. Consequently, the RGA and the RNGA can be calculated by [14]:

$$RGA = [\lambda_{ij}]_{n\times n} = K \otimes (K)^{-T} \quad (38)$$

$$RNGA = [\phi_{ij}]_{n\times n} = (K \odot E) \otimes (K \odot E)^{-T} \quad (39)$$

where $\otimes$ and $\odot$ are element-by-element product and division, respectively, $(\cdot)^{-T}$ is inverse and transpose. The definitions of relative gain λ_{ij}'s and relative normalized gains ϕ_{ij}'s are [14]:

$$\lambda_{ij} = \frac{k_{ij}}{\hat{k}_{ij}},\ \phi_{ij} = \frac{k_{ij}/e_{ij}}{\hat{k}_{ij}/\hat{e}_{ij}} = \frac{k_{ij}}{\hat{k}_{ij}}\cdot\frac{\hat{e}_{ij}}{e_{ij}} = \lambda_{ij}\cdot\gamma_{ij} \quad (40)$$

where $\gamma_{ij} = \hat{e}_{ij}/e_{ij}$ is called relative normalized integrated error, $\hat{k}_{ij}$ and $\hat{e}_{ij}$ are the apparent steady-state gain and normalized integrated error of $y_i - u_j$ when other loops are closed [14]. ϕ_{ij} reflects the total effect imposed on y_i by u_j through including both k_{ij} and e_{ij}. Note that the sum of the elements in each column/row of RGA and RNGA is 1.

The rules to pair inputs and outputs to determine a $\overline{F}_{TS}$ for choosing decentralized control configuration are [14]:

i). *λ_{ij}'s and ϕ_{ij}'s of all paired elements are positive*;

ii). *ϕ_{ij}'s of paired elements should be closest to 1*;

iii). $NI = det(K)\,/\prod_{i=1}^{n} k_{ii} > 0$.

where $\det(K)$ is the determinant of K after swapping the columns to place the pairs in the diagonal positions if necessary, and $\prod_{i=1}^{n} k_{ii}$ is the product of the steady-state gains of the paired channels. A positive NI is a necessary condition for a stable control system [8],[13]-[15],[17].

Remark 3.2: The values of λ_{ij} and ϕ_{ij} reflect the changes of steady and dynamic properties of $y_i - u_j$ when other loops are closed. According to (40), it is easy to learn that the closer λ_{ij} and ϕ_{ij} to 1, the less the steady-state gain and the normalized integrated error of $y_i - u_j$ will change, which means the smaller interacting effects $y_i - u_j$ will receive from other channels, and thus $y_i - u_j$ is with higher degree of independence and dominance. Note that λ_{ij} and ϕ_{ij} can be derived only using individual open-loop model $f_{TS,ij}$.

Swapping the columns of F_{TS} to place the paired elements on the diagonal positions if necessary, $\overline{F}_{TS}$ for sparse control configuration can be expressed by:

$$\overline{F}_{TS} = \begin{bmatrix} f_{TS,11} & \vartheta_{12}f_{TS,12} & \cdots & \vartheta_{1n}f_{TS,1n} \\ \vartheta_{21}f_{TS,21} & f_{TS,22} & \cdots & \vartheta_{2n}f_{TS,2n} \\ \vdots & \vdots & \ddots & \vdots \\ \vartheta_{n1}f_{TS,n1} & \vartheta_{n2}f_{TS,n2} & \cdots & f_{TS,nn} \end{bmatrix} \quad (41)$$

where $\vartheta_{ij} = 1$ or 0. We propose two interaction indexes, denoted by $\mathcal{A} = [\alpha_{ij}]_{n\times n}$ and $\mathcal{B} = [\beta_{ij}]_{n\times n}$, to determine ϑ_{ij}:

$$\alpha_{ij} = \frac{1}{2}\times\left(\frac{|\lambda_{ij}|}{|\lambda_{ii}|} + \frac{|\lambda_{ij}|}{|\lambda_{jj}|}\right) \quad (42)$$

$$\beta_{ij} = \frac{1}{2}\times\left(\frac{|\phi_{ij}|}{|\phi_{ii}|} + \frac{|\phi_{ij}|}{|\phi_{jj}|}\right) = \frac{1}{2}\times\left(\frac{|\lambda_{ij}|}{|\lambda_{ii}|}\cdot\frac{|\gamma_{ij}|}{|\gamma_{ii}|} + \frac{|\lambda_{ij}|}{|\lambda_{jj}|}\cdot\frac{|\gamma_{ij}|}{|\gamma_{jj}|}\right) \quad (43)$$

Equations (42)-(43) imply that if both α_{ij} and β_{ij} are close to 1, the changes of steady and dynamic properties of $y_i - u_j$ are similar to that of paired channels $y_i - u_i$ and $y_j - u_j$, which means $y_i - u_j$ receives relatively small coupling effects and has relatively large degree of independence and dominance. Given ε_α and ε_β that $0 \le \varepsilon_\alpha, \varepsilon_\beta \le 1$, the following criterion can be used to determine the value of ϑ_{ij} in (41):

$$\vartheta_{ij}=\begin{cases}1, & if\ \varepsilon_\alpha\le\alpha_{ij}\le 1/\varepsilon_\alpha\ and\ \varepsilon_\beta\le\beta_{ij}\le 1/\varepsilon_\beta\\ 0, & else\end{cases} \tag{44}$$

Note that when $\varepsilon_\alpha,\varepsilon_\beta=0$, all the ϑ_{ij}'s are 1 to select a full-dimensional control configuration; when $\varepsilon_\alpha,\varepsilon_\beta=1$, all the ϑ_{ij}'s are 0 to remain the 1-for-1 decentralized control. The smaller ε_α and ε_β are, the richer the control configuration will be. According to experience, generally, the values of ε_α and ε_β are chosen from [0.1, 0.3].

Remark 3.3: Reference [15] proposed a method that only using the values of $|\phi_{ij}|/|\phi_{ii}|=(|\lambda_{ij}|/|\lambda_{ii}|)\cdot(|\gamma_{ij}|/|\gamma_{ii}|)$ to assess the relative dominance that the unpaired elements satisfying one or more of the following conditions should NOT be selected: i). $|\lambda_{ij}|/|\lambda_{ii}|$ is very large; ii). $|\lambda_{ij}|/|\lambda_{ii}|$ is very small; iii). $|\gamma_{ij}|/|\gamma_{ii}|$ is very large; iv). $|\gamma_{ij}|/|\gamma_{ii}|$ is very small. Thus the unpaired element with moderate value of $|\phi_{ij}|/|\phi_{ii}|$ (in [0.15, 8]) should be considered for sparse control. However, a channel with moderate $|\phi_{ij}|/|\phi_{ii}|$ may have very large $|\lambda_{ij}|/|\lambda_{ii}|$ and very small $|\gamma_{ij}|/|\gamma_{ii}|$, or very small $|\lambda_{ij}|/|\lambda_{ii}|$ and very large $|\gamma_{ij}|/|\gamma_{ii}|$, which means the method in [15] may select inappropriate sparse control configurations. In this paper, α_{ij} and β_{ij} consider both RGA and RNGA and compare the effects of all inputs on y_i as well as the effects of u_j on all outputs to offer a safer and more reasonable result.

C. Sensitivities of the two interaction measures

The sensitivities of the two interaction measures with respect to the parametric variations of $f_{TS,ij}$ $(i,j=1,\cdots,n)$ can be used to compare the robustness of the two measures and see whether their decisions on control configurations will change or not under the influence of parametric uncertainties. Based on an operating point given in (15), suppose the parameters of the model in (16) are varying in the following ranges:

$$\begin{aligned}&a_{ij,r}\in[a_{ij,r}-\Delta a_{ij,r},\ a_{ij,r}+\Delta a_{ij,r}],\Delta a_{ij,r}\ge 0,r=1,\cdots,p\\&b_{ij,s}\in[b_{ij,s}-\Delta b_{ij,s},\ b_{ij,s}+\Delta b_{ij,s}],\Delta b_{ij,s}\ge 0,s=0,1,\cdots,q\\&\tau_{ij}\in[\tau_{ij}-\Delta\tau_{ij},\ \tau_{ij}+\Delta\tau_{ij}],\Delta\tau_{ij}\ge 0\end{aligned} \tag{45}$$

As a result, there will be variations in the elements of PM (ψ_{ij}), RGA (λ_{ij}) and RNGA (ϕ_{ij}) as follows:

$$\begin{aligned}&\psi_{ij}\in[\psi_{ij}-\Delta\psi_{ij},\quad \psi_{ij}+\Delta\psi_{ij}],\Delta\psi_{ij}\ge 0\\&\lambda_{ij}\in[\lambda_{ij}-\Delta\lambda_{ij},\quad \lambda_{ij}+\Delta\lambda_{ij}],\Delta\lambda_{ij}\ge 0\\&\phi_{ij}\in[\phi_{ij}-\Delta\phi_{ij},\quad \phi_{ij}+\Delta\phi_{ij}],\Delta\phi_{ij}\ge 0\end{aligned} \tag{46}$$

Knowing the values of $\Delta\psi_{ij}$, $\Delta\lambda_{ij}$ and $\Delta\phi_{ij}$, we can determine whether the selected elements varying in the ranges of (46) will remain dominant or not in PM, RGA and RNGA, and then deduce whether the configurations will be the same or may change under the parametric uncertainties in (45).

This subsection introduces sensitivity calculations to derive $\Delta\psi_{ij}$, $\Delta\lambda_{ij}$ and $\Delta\phi_{ij}$. For the PM in (25), the partial derivative $\partial\psi_{ij}/\partial tr_{rs}$ $(i,j,r,s=1,\cdots,n)$ can be obtained by:

$$\frac{\partial\psi_{ij}}{\partial tr_{rs}}=\begin{cases}(1-\psi_{ij})\psi_{ij}/tr_{ij}, & i=r\ and\ j=s\\ -\psi_{ij}^2/tr_{ij} & i\ne r\ or\ j\ne s\end{cases} \tag{47}$$

For the RGA in (38), $\partial\lambda_{ij}/\partial k_{rs}$ can be obtained by [29]:

$$\frac{\partial\lambda_{ij}}{\partial k_{rs}}=\begin{cases}\lambda_{ij}(1-\lambda_{ij})/k_{ij}, & i=r\ and\ j=s\\ -\lambda_{ij}\lambda_{rs}/k_{rs}, & i=r\ or\ j=s\\ \frac{(-1)^{i+j+r+s}k_{ij}\det(K_{ij,rs})}{\det(K)}-\frac{\lambda_{ij}\lambda_{rs}}{k_{rs}} & i\ne r\ and\ j\ne s\end{cases} \tag{48}$$

where $(\cdot)_{ij,rs}$ denotes the submatrix of $(\cdot)$ with rows i and r and columns j and s removed. Similarly, for RNGA in (39), denote $\overline{k}_{rs}=k_{rs}/e_{rs}$ and $\overline{K}=\left[\overline{k}_{ij}\right]_{n\times n}$, and then $\partial\phi_{ij}/\partial\overline{k}_{rs}$ can be obtained using (48) where λ_{ij}, k_{ij}, K and $K_{ij,rs}$ are replaced by ϕ_{ij}, $\overline{k}_{ij}$, $\overline{K}$ and $\overline{K}_{ij,rs}$ respectively.

The $f_{TS,ij}$ with $p=2$ and $q=0$ is chosen to investigate the sensitivities. For PM, from (27) we can have:

$$\begin{cases}\frac{\partial tr_{ij}}{\partial a_{ij,1}}=\frac{\partial\Upsilon}{\partial a_{ij,1}}\cdot\frac{b_{ij,0}^2}{\Omega^2}-\frac{\partial\Omega}{\partial a_{ij,1}}\cdot\frac{2\Upsilon b_{ij,0}^2}{\Omega^3}-\frac{\partial\Omega}{\partial a_{ij,1}}\cdot\frac{\tau_{ij}(1-a_{ij,2})}{\Omega^2/b_{ij,0}^2},\\ \frac{\partial tr_{ij}}{\partial a_{ij,2}}=\frac{\partial\Upsilon}{\partial a_{ij,2}}\cdot\frac{b_{ij,0}^2}{\Omega^2}-\frac{\partial\Omega}{\partial a_{ij,2}}\cdot\frac{2\Upsilon b_{ij,0}^2}{\Omega^3}-\frac{\partial\Omega}{\partial a_{ij,2}}\cdot\frac{\tau_{ij}\Omega+\tau_{ij}(1-a_{ij,2})}{\Omega^2/b_{ij,0}^2},\\ \frac{\partial tr_{ij}}{\partial b_{ij,0}}=\frac{2tr_{ij}}{b_{ij,0}},\quad \frac{\partial tr_{ij}}{\partial\tau_{ij}}=\frac{b_{ij,0}^2\times(1-a_{ij,2})}{\Omega}.\end{cases} \tag{49}$$

where $\Omega=[(1-a_{ij,2})^2-a_{ij,1}^2](1+a_{ij,2})$, $\Upsilon=(1-a_{ij,2})^2(1+a_{ij,2}^2)+2a_{ij,1}^2a_{ij,2}$, $\partial\Omega/\partial a_{ij,1}=-2a_{ij,1}(1+a_{ij,2})$, $\partial\Omega/\partial a_{ij,2}=[(1-a_{ij,2})^2-a_{ij,1}^2]-2(1-a_{ij,2})(1+a_{ij,2})$, $\partial\Upsilon/\partial a_{ij,1}=4a_{ij,1}a_{ij,2}$, $\partial\Upsilon/\partial a_{ij,2}=2[a_{ij,2}(1-a_{ij,2})^2-(1+a_{ij,2}^2)(1-a_{ij,2})+a_{ij,1}^2]$. Then $\Delta\psi_{ij}$ can be calculated using Taylor's series truncating after the first order terms:

$$\Delta\psi_{ij}\cong\sum_{r=1}^{n}\sum_{s=1}^{n}\left(\left|\frac{\partial\psi_{ij}}{\partial tr_{rs}}\cdot\frac{\partial tr_{rs}}{\partial a_{rs,1}}\right|\Delta a_{rs,1}+\left|\frac{\partial\psi_{ij}}{\partial tr_{rs}}\cdot\frac{\partial tr_{rs}}{\partial a_{rs,2}}\right|\Delta a_{rs,2}+\left|\frac{\partial\psi_{ij}}{\partial tr_{rs}}\cdot\frac{\partial tr_{rs}}{\partial b_{rs,0}}\right|\Delta b_{rs,0}+\left|\frac{\partial\psi_{ij}}{\partial tr_{rs}}\cdot\frac{\partial tr_{rs}}{\partial\tau_{rs}}\right|\Delta\tau_{rs}\right)\Big|_{x_{ij}(k_0),\ i,j=1,\cdots,n} \tag{50}$$

For RGA and RNGA, from (36)-(37), we have:

$$\begin{cases}\frac{\partial k_{ij}}{\partial a_{ij,1}}=\frac{\partial k_{ij}}{\partial a_{ij,2}}=-\frac{k_{ij}^2}{b_{ij,0}},\quad \frac{\partial k_{ij}}{\partial b_{ij,0}}=\frac{k_{ij}}{b_{ij,0}},\quad \frac{\partial k_{ij}}{\partial\tau_{ij}}=0\end{cases} \tag{51}$$

$$\begin{cases}\frac{\partial\overline{k}_{ij}}{\partial a_{ij,1}}=\frac{-k_{ij}^2(2e_{ij}-(\tau_{ij}-1)\cdot T)}{b_{ij,0}\times e_{ij}^2},\quad \frac{\partial\overline{k}_{ij}}{\partial a_{ij,2}}=\frac{-k_{ij}^2(2e_{ij}-(\tau_{ij}-2)\cdot T)}{b_{ij,0}\times e_{ij}^2},\\ \frac{\partial\overline{k}_{ij}}{\partial b_{ij,0}}=\frac{k_{ij}}{b_{ij,0}\times e_{ij}},\qquad \frac{\partial\overline{k}_{ij}}{\partial\tau_{ij}}=\frac{-k_{ij}\times T}{e_{ij}^2}\end{cases} \tag{52}$$

Similar to (50), $\Delta\lambda_{ij}$ and $\Delta\phi_{ij}$ are calculated by:

$$\Delta\lambda_{ij}\cong\sum_{r=1}^{n}\sum_{s=1}^{n}\left(\left|\frac{\partial\lambda_{ij}}{\partial k_{rs}}\cdot\frac{\partial k_{rs}}{\partial a_{rs,1}}\right|\Delta a_{rs,1}+\left|\frac{\partial\lambda_{ij}}{\partial k_{rs}}\cdot\frac{\partial k_{rs}}{\partial a_{rs,2}}\right|\Delta a_{rs,2}+\left|\frac{\partial\lambda_{ij}}{\partial k_{rs}}\cdot\frac{\partial k_{rs}}{\partial b_{rs,0}}\right|\Delta b_{rs,0}\right)\Big|_{x_{ij}(k_0),\ i,j=1,\cdots,n} \tag{53}$$

$$\Delta\phi_{ij}\cong\sum_{r=1}^{n}\sum_{s=1}^{n}\left(\left|\frac{\partial\phi_{ij}}{\partial\overline{k}_{rs}}\cdot\frac{\partial\overline{k}_{rs}}{\partial a_{rs,1}}\right|\Delta a_{rs,1}+\left|\frac{\partial\phi_{ij}}{\partial\overline{k}_{rs}}\cdot\frac{\partial\overline{k}_{rs}}{\partial a_{rs,2}}\right|\Delta a_{rs,2}+\left|\frac{\partial\phi_{ij}}{\partial\overline{k}_{rs}}\cdot\frac{\partial\overline{k}_{rs}}{\partial b_{rs,0}}\right|\Delta b_{rs,0}+\left|\frac{\partial\phi_{ij}}{\partial\overline{k}_{rs}}\cdot\frac{\partial\overline{k}_{rs}}{\partial\tau_{rs}}\right|\Delta\tau_{rs}\right)\Big|_{x_{ij}(k_0),\ i,j=1,\cdots,n} \tag{54}$$

IV. Discussion

A qualified interaction measure for control configuration selection should, firstly, consider sufficient information of the multivariable process and use reasonable rules to determine the dominant channels for both decentralized and sparse control;

secondly, be robust to uncertainties, i.e., the decisions on control configuration are not easy to change under the influence of uncertainties within a certain range; thirdly, satisfy necessary condition for stable controller development; and lastly, be able to provide useful information, such as the quantified interactions among the channels, to facilitate the following controller design.

The two interaction measures studied in this paper utilize different concepts to select control configurations. Gramian-based method grants the channels with states easy to control and observe high degree of dominance, while RNGA chooses the channels with high independence that have strong immunity to the coupling effects from other closed-loops. The manners used by both of them in control configuration selection are plausible and meaningful. In the previous studies [2]-[4], it was stated that gramian-based methods are superior to RGA family mainly because **i)**. RGA only considers the process at one particular frequency, while gramians take the whole frequency range into account; **ii)**. RGA is not sensitive to time delays, while the calculations of gramians include time delays; **iii)**. RGA can only determine pairing structure for decentralized control, while gramians can select both decentralized and sparse control configurations. Nevertheless, by considering normalized integrated error together with steady-state gain, RNGA as a member of RGA family overcomes these drawbacks: **i)**. RNGA covers the whole frequency domain; **ii)**. RNGA considers the dynamic properties of the process, including time delays; **iii)**. the proposed two interaction indexes $\mathcal{A}$ and $\mathcal{B}$ defined from RGA and RNGA provide a reasonable criterion for sparse control configuration selection. Therefore, at present, it is inappropriate to state that gramian-based methods are superior to RGA family.

On the other hand, the dominant channels selected by RNGA are more independent and less affected by the coupling effects than the rest channels. Therefore, compared to the PM in (25), the values in RGA and RNGA for the selected elements should be more robust to the coupling and disturbances from other channels, and the control configurations determined by RNGA based interaction measure should be less prone to change than that determined by gramians under the influence of parametric uncertainties.

Besides, RGA family takes NI [8] introduced in the subsection *B* of Section III as a complementary tool to pair inputs and outputs for decentralized control. NI is a necessary condition for stability that, if NI is negative, the multivariable closed-loop control system will be instable for all possible (any) values of controller parameters (i.e., it will be "structurally monotonic instable") [8],[13]-[15],[17]. In contrast, no such type of index to guarantee the necessary condition of a stable controller is included in gramian-based measures.

In addition, RGA family can provide the steady and dynamic properties of each channel when other loops are closed, such as the $\hat{k}_{ij}$ and the $\hat{e}_{ij}$ of RGA and RNGA in (40). By virtue of this special skill, the interaction measures in this category can not only be used to determine control configurations, but also be employed to simplify the subsequent multivariable controller design. Currently, several studies can be found that using dynamic RGA, effective relative gain array and RNGA to construct a group of so-called "effective models" [15],[22],[28],[30],[31] to describe a batch of equivalent non-interacting SISO processes to represent an MIMO process, such that the multivariable controller design can be decomposed into multiple independent single-loop control system designs. In contrast, the PM cannot provide such type of information. The existing studies of gramian-based interaction measures [1]-[6],[9] only present the results of control configuration selection, and do not give any explicit description of how to use the quantified interactions for the following decentralized or sparse control system design.

V. CASE STUDIES

A. Example I

Consider a 3×3 process [14] with the transfer functions as:

$$G(s) = \begin{bmatrix} \frac{e^{-9s}}{6s^2+17s+1} & \frac{-9e^{-5s}}{s^2+4s+1} & \frac{13e^{-3s}}{3s^2+35s+1} \\ \frac{-5e^{-13s}}{2s^2+19s+1} & \frac{8e^{-2s}}{s^2+33s+1} & \frac{7e^{-5s}}{s^2+3s+1} \\ \frac{-16e^{-3s}}{s^2+5s+1} & \frac{3e^{-7s}}{s^2+14s+1} & \frac{e^{-11s}}{3s^2+25s+1} \end{bmatrix} \tag{55}$$

Choose sampling time as $T = 1s$, and suppose there are noises random but bounded in $[-0.1,\ 0.1]$ in the input signals. For each channel, choose $L_{ij} = 4$, $p = 2$ and $q = 0$ for its fuzzy models, collect the input-output data samples and use the identification method presented in Section II to build a type-1 fuzzy model, and then extend it to type-2. Due to the limited space, we only present the first rules in the two types of fuzzy models for $y_1 - u_1$:

Type-1 fuzzy rule 1: if $x_{11}(k)$ is Z_{11}^1, then
$y_1^1(k) = 1.3397y_1(k-1) - 0.3796y_1(k-2) + 0.0389u_1(k-9)$

Type-2 fuzzy rule 1: if $x_{11}(k)$ is $\tilde{Z}_{11}^1$, then
$\tilde{y}_1^1(k) = [1.6248, 1.0545]y_1(k-1) - [0.6900, 0.0692]y_1(k-2) + [0.0418, 0.0359]u_1(k-9)$

The center of $Z_{11}^1/\tilde{Z}_{11}^1$ is $xc^l = [1.0337\ \ 1.0165\ \ 1.0452]^T$, and $\Delta\mu^1 = 0.0999$.

Table I. The comparisons of the two types of fuzzy models for (55)

	Original process	Type-1 fuzzy model	Type-2 fuzzy model
RMSE	——	$\begin{bmatrix} 0.0035 & 0.0681 & 0.0015 \\ 0.0015 & 0.0001 & 0.1101 \\ 0.0643 & 0.0005 & 0.0003 \end{bmatrix}$	$\begin{bmatrix} 0.0021 & 0.0416 & 0.0007 \\ 0.0008 & 0.00006 & 0.0674 \\ 0.0402 & 0.0003 & 0.0001 \end{bmatrix}$
TR	$\begin{bmatrix} 0.5354 & 76.5987 & 50.9777 \\ 15.1464 & 18.4318 & 57.7576 \\ 156.2948 & 4.6728 & 0.4824 \end{bmatrix}$	$\begin{bmatrix} 0.5711 & 80.2055 & 50.9741 \\ 15.2826 & 18.4570 & 62.1774 \\ 160.9928 & 4.6976 & 0.4854 \end{bmatrix}$	$\begin{bmatrix} 0.5695 & 77.9277 & 50.9743 \\ 15.2789 & 18.4562 & 60.0446 \\ 159.8412 & 4.6884 & 0.4854 \end{bmatrix}$
PM	$\begin{bmatrix} 0.0014 & 0.2011 & 0.1338 \\ 0.0398 & 0.0484 & 0.1516 \\ 0.4103 & 0.0123 & 0.0013 \end{bmatrix}$	$\begin{bmatrix} 0.0015 & 0.2036 & 0.1294 \\ 0.0388 & 0.0469 & 0.1579 \\ 0.4088 & 0.0119 & 0.0012 \end{bmatrix}$	$\begin{bmatrix} 0.0015 & 0.2007 & 0.1313 \\ 0.0394 & 0.0475 & 0.1546 \\ 0.4117 & 0.0121 & 0.0013 \end{bmatrix}$
Paired elements (Gramians)	$y_1 - u_2/y_2 - u_3/y_3 - u_1$	$y_1 - u_2/y_2 - u_3/y_3 - u_1$	$y_1 - u_2/y_2 - u_3/y_3 - u_1$
K	$\begin{bmatrix} 1 & -9 & 13 \\ -5 & 8 & 7 \\ -16 & 3 & 1 \end{bmatrix}$	$\begin{bmatrix} 0.9979 & -8.8870 & 12.9979 \\ -4.9990 & 7.9990 & 6.9288 \\ -15.8996 & 2.9997 & 0.9997 \end{bmatrix}$	$\begin{bmatrix} 1.0000 & -9.0634 & 12.9982 \\ -5.0003 & 7.9998 & 7.0699 \\ -16.0919 & 3.0001 & 0.9998 \end{bmatrix}$
E	$\begin{bmatrix} 26 & 9 & 38 \\ 32 & 35 & 8 \\ 8 & 21 & 36 \end{bmatrix}$	$\begin{bmatrix} 23.8638 & 8.2298 & 37.2323 \\ 31.2678 & 34.4714 & 7.1726 \\ 7.2794 & 20.4265 & 35.0998 \end{bmatrix}$	$\begin{bmatrix} 24.0455 & 8.4671 & 37.2396 \\ 31.2702 & 34.4740 & 7.3882 \\ 7.4329 & 20.4280 & 35.1048 \end{bmatrix}$
RGA	$\begin{bmatrix} -0.0054 & 0.3981 & 0.6073 \\ -0.0992 & 0.6912 & 0.4080 \\ 1.1046 & -0.0893 & -0.0153 \end{bmatrix}$	$\begin{bmatrix} -0.0054 & 0.3927 & 0.6127 \\ -0.1006 & 0.6979 & 0.4026 \\ 1.1059 & -0.0906 & -0.0153 \end{bmatrix}$	$\begin{bmatrix} -0.0054 & 0.4022 & 0.6032 \\ -0.0980 & 0.6860 & 0.4121 \\ 1.1034 & -0.0882 & -0.0152 \end{bmatrix}$
$RNGA$	$\begin{bmatrix} -0.0024 & 0.9237 & 0.0787 \\ -0.0063 & 0.0829 & 0.9235 \\ 1.0088 & -0.0066 & -0.0022 \end{bmatrix}$	$\begin{bmatrix} -0.0023 & 0.9331 & 0.0693 \\ -0.0054 & 0.0727 & 0.9327 \\ 1.0077 & -0.0058 & -0.0019 \end{bmatrix}$	$\begin{bmatrix} -0.0023 & 0.9319 & 0.0704 \\ -0.0055 & 0.0740 & 0.9315 \\ 1.0079 & -0.0059 & -0.0019 \end{bmatrix}$
Paired elements (RNGA)	$y_1 - u_2/y_2 - u_3/y_3 - u_1$	$y_1 - u_2/y_2 - u_3/y_3 - u_1$	$y_1 - u_2/y_2 - u_3/y_3 - u_1$
$\mathcal{A}$	$\begin{bmatrix} 0.0092 & 1 & 1.5069 \\ 0.1665 & 1.7151 & 1 \\ 1 & 0.1526 & 0.0257 \end{bmatrix}$	$\begin{bmatrix} 0.0093 & 1 & 1.5409 \\ 0.1703 & 1.7553 & 1 \\ 1 & 0.1563 & 0.0259 \end{bmatrix}$	$\begin{bmatrix} 0.0091 & 1 & 1.4817 \\ 0.1634 & 1.6851 & 1 \\ 1 & 0.1496 & 0.0254 \end{bmatrix}$
$\mathcal{B}$	$\begin{bmatrix} 0.0025 & 1 & 0.0852 \\ 0.0066 & 0.0897 & 1 \\ 1 & 0.0068 & 0.0022 \end{bmatrix}$	$\begin{bmatrix} 0.0024 & 1 & 0.0742 \\ 0.0056 & 0.0780 & 1 \\ 1 & 0.0060 & 0.0020 \end{bmatrix}$	$\begin{bmatrix} 0.0024 & 1 & 0.0756 \\ 0.0057 & 0.0794 & 1 \\ 1 & 0.0061 & 0.0020 \end{bmatrix}$

The root-mean-square errors (RMSEs) of the two types of fuzzy model and the calculated results (given the operating points as $x_{ij}(k_0) = [0\ 0\ 0]^T$ for $i,j = 1,2,3$) for interaction measure are shown and compared in Table I. It can be seen that compared to type-1 fuzzy models, IT2TSF models reduce the RMSEs up to 66%, and achieve higher accuracy in calculating K, E and TR. The paired elements for decentralized control selected by two interaction measures are same: $y_1 - u_2/y_2 - u_3/y_3 - u_1$. In addition, both RNGA (using $\varepsilon_\alpha = \varepsilon_\beta = 0.1$) and gramians suggest that sparse control is not necessary for this MIMO process.

Suppose there are parametric variations in $b_{ij,0}$ of (16) with the varying radiuses as $\Delta b_{ij,0} = 20\% \times |b_{ij,0}|$ for $i,j = 1,2,3$, then the varying ranges of the elements in PM, RGA and RNGA as shown in (46) can be calculated based on IT2TSF models using equations (50), (53) and (54):

$$PM = \left[[\psi_{ij} - \Delta\psi_{ij}, \psi_{ij} + \Delta\psi_{ij}]\right]_{3\times3} = \begin{bmatrix} [0.0003,\ 0.0026] & [0.0724,\ 0.3290] & [0.0400,\ 0.2225] \\ [0.0091,\ 0.0696] & [0.0113,\ 0.0838] & [0.0501,\ 0.2592] \\ [0.2179,\ 0.6054] & [0.0025,\ 0.0216] & [0.0003,\ 0.0022] \end{bmatrix} \quad (56)$$

$$RGA = \left[[\lambda_{ij} - \Delta\lambda_{ij}, \lambda_{ij} + \Delta\lambda_{ij}]\right]_{3\times3} = \begin{bmatrix} [-0.0140,\ 0.0032] & [0.0049,\ 0.7995] & [-0.0887,\ 1.2950] \\ [-0.2238,\ 0.0277] & [-0.0057,\ 1.3777] & [0.0117,\ 0.8125] \\ [0.1294,\ 2.0775] & [-0.2014,\ 0.0249] & [-0.0349,\ 0.0044] \end{bmatrix} \quad (57)$$

$$RNGA = \left[[\phi_{ij} - \Delta\phi_{ij}, \phi_{ij} + \Delta\phi_{ij}]\right]_{3\times3} = \begin{bmatrix} [-0.0044,\ -0.0003] & [0.5015,\ 1.3624] & [-0.0153,\ 0.1561] \\ [-0.0121,\ 0.0011] & [-0.0131,\ 0.1610] & [0.5011,\ 1.3620] \\ [0.1952,\ 1.8205] & [-0.0130,\ 0.0012] & [-0.0036,\ -0.0002] \end{bmatrix} \quad (58)$$

From (56) it can be seen that, under the influence of the parametric uncertainties, the PM elements for $y_1 - u_3$ and $y_2 - u_3$ have similar varying ranges, which implies it is possible that $y_1 - u_3$ replaces $y_2 - u_3$ to be a paired element. For example, PM with the varying ranges indicated in (56) may become:

$$PM = \begin{bmatrix} 0.0016 & 0.1 & 0.21 \\ 0.04 & 0.075 & 0.06 \\ 0.5 & 0.0121 & 0.0013 \end{bmatrix}$$

Then the pairing structure determined by PM changes to $y_1 - u_3/y_2 - u_2/y_3 - u_1$. In contrast, (57) and (58) demonstrate that the pairing structure selected by RNGA based measure will be unchanged since the λ_{ij}'s and the ϕ_{ij}'s of the paired channels $(y_1 - u_2/y_2 - u_3/y_3 - u_1)$ always have dominant values in their varying ranges.

B. Example II

Consider a 3 × 3 nonlinear process [22] as follows:

$$\begin{aligned} \dot{x}_1 &= x_2 + 5x_1^2x_2 + 6x_2^2 \\ \dot{x}_2 &= -4x_1 - 5x_2 + 8x_1x_2 + u_1 \\ \dot{x}_3 &= x_4 \\ \dot{x}_4 &= -6x_3 - 5x_4 + 3x_3^3 + 10x_3x_4x_5 + u_2 \\ \dot{x}_5 &= x_6 + 4x_7^2 \\ \dot{x}_6 &= x_7 + 5x_5x_6^2x_7 \\ \dot{x}_7 &= -14x_5 - 23x_6 - 10x_7 + 7x_5x_6x_7 + u_3 \\ y_1 &= 5x_1 + 5x_2 + 6x_3 + 2x_4 + 14x_5 + 9x_6 + x_7 \\ y_2 &= 8x_1 + 2x_2 + 3x_3 + 4x_5 + 6x_6 + 2x_7 \end{aligned}$$

$$y_3 = x_1 + x_2 + 4x_3 + 2x_4 + 1.4x_5 + 0.2x_6 \quad (59)$$

where x_v's $(v = 1, \cdots, 7)$ are states. The time delays are $\tau'_{i1} = \tau'_{i2} = 2$ (sec) and $\tau'_{i3} = 1$ (sec) for $i = 1,2,3$, choose $T = 0.1s$. For each input-output channel, the fuzzy models are constructed with $L_{ij} = 6$, $p = 2$ and $q = 0$. The comparison of RMSEs between the two types of fuzzy model for each channel is shown in Table II, which demonstrates that IT2TSF models are of higher accuracy compared to their type-1 counterparts.

Table II. The RMSEs of the two types of fuzzy models for (59)

	Type-1	Type-2
RMSE	$\begin{bmatrix} 0.0031 & 1.01\times10^{-5} & 0.0047 \\ 0.0169 & 0.0051 & 0.0014 \\ 6.19\times10^{-4} & 1.15\times10^{-5} & 7.6973\times10^{-4} \end{bmatrix}$	$\begin{bmatrix} 0.0020 & 5.23\times10^{-6} & 0.0028 \\ 0.0110 & 0.0028 & 8.15\times10^{-4} \\ 4.93\times10^{-4} & 6.62\times10^{-6} & 7.6950\times10^{-4} \end{bmatrix}$

We only present the first fuzzy rule of the IT2TSF model for $y_1 - u_1$ due to the limited space:

Rule 1: if $x_{11}(k)$ is $\tilde{Z}_{11}^1$, then
$\tilde{y}_1^1(k) = [0.6492, 0.6408]y_1(k-1) +$
$[-0.0081, 0.0042]y_1(k-2) + [0.4134, 0.3945]u_1(k-20)$

The center of $\tilde{Z}_{11}^1$ is $xc^l = [-0.3158\ -0.1533\ 0.0503]^T$, and $\Delta\mu^1 = 0.0995$. Given the operating points as $x_{ij}(k_0) = [0\ 0\ 0]^T$ for $i,j = 1,2,3$, the calculated results of the two measures from IT2TSF models are:

$$TR = \begin{bmatrix} 6.6742 & 2.2603 & 0.8019 \\ 6.2057 & 0.3942 & 0.3105 \\ 0.2608 & 1.4705 & 0.0047 \end{bmatrix}, \quad PM = \begin{bmatrix} 0.3631 & 0.1230 & 0.0436 \\ 0.3376 & 0.0214 & 0.0169 \\ 0.0142 & 0.0800 & 0.0003 \end{bmatrix}$$

$$K = \begin{bmatrix} 1.2405 & 1.0003 & 1.0049 \\ 2.2379 & 0.4956 & 0.2861 \\ 0.2420 & 0.6669 & 0.0958 \end{bmatrix}, \quad E = \begin{bmatrix} 2.2013 & 2.4518 & 1.9160 \\ 2.9957 & 2.7888 & 1.0991 \\ 2.1944 & 2.2860 & 3.7368 \end{bmatrix}$$

$$RGA = \begin{bmatrix} -0.1683 & -0.1375 & 1.3058 \\ 1.2169 & -0.0583 & -0.1585 \\ -0.0485 & 1.1958 & -0.1473 \end{bmatrix}, \quad \mathcal{A} = \begin{bmatrix} 0.1336 & 0.1101 & 1 \\ 1 & 0.0484 & 0.1258 \\ 0.0402 & 1 & 0.1180 \end{bmatrix}$$

$$RNGA = \begin{bmatrix} -0.5942 & 0.0576 & 1.5366 \\ 1.5731 & -0.1139 & -0.4591 \\ 0.0212 & 1.0563 & -0.0775 \end{bmatrix}, \quad \mathcal{B} = \begin{bmatrix} 0.3822 & 0.0460 & 1 \\ 1 & 0.0901 & 0.2953 \\ 0.0167 & 1 & 0.0619 \end{bmatrix}$$

According to the above arrays, both RNGA (using $\varepsilon_\alpha = \varepsilon_\beta = 0.1$) and gramians suggest sparse control for this MIMO process. The two measures select the same pairing structure: $y_1 - u_3/y_2 - u_1/y_3 - u_2$ for decentralized control, but different unpaired element(s) for sparse control: gramians choose $y_1 - u_1$ while RNGA chooses $y_1 - u_1$ and $y_2 - u_3$. We employ the independent design method [15],[28] together with effective fuzzy model [22] to devise controllers for this MIMO process to compare these different configurations. The independent design method [15],[28] converts a multivariable control system design to multiple independent SISO controller designs based on the effective fuzzy models [22] of the selected dominant channels. The gain and phase margins based control algorithm [22] is used to design each SISO controller with the same required gain margin (set as 3) and phase margin (set as $\pi/3$) to provide a fair comparison between the two measures. Given the reference values as $rv_1 = 0.3$, $rv_2 = 1$ and $rv_3 = 0$, the results are shown in Fig. 2, from which it can be seen that the sparse control with the configuration containing one more unpaired element ($y_2 - u_3$) selected by RNGA eliminates the overshoot in y_1 and achieves much smaller overshoot in y_3 compared to the decentralized control, while the difference between decentralized and sparse control with the configuration selected by gramians are miniscule.

Suppose there are parametric variations in $b_{ij,0}$ of (16) with the varying radiuses as $\Delta b_{ij,0} = 10\% \times |b_{ij,0}|$ for $i,j = 1,2,3$, then the varying ranges of the elements in PM, RGA and RNGA can be calculated and are given in (60)-(62):

$$PM = [[\psi_{ij} - \Delta\psi_{ij}, \psi_{ij} + \Delta\psi_{ij}]]_{3\times3} = \begin{bmatrix} [0.2706,\ 0.4556] & [0.0798,\ 0.1661] & [0.0269,\ 0.0603] \\ [0.2481,\ 0.4270] & [0.0131,\ 0.0298] & [0.0102,\ 0.0235] \\ [0.0086,\ 0.0198] & [0.0506,\ 0.1094] & [0.0002,\ 0.0004] \end{bmatrix} \quad (60)$$

$$RGA = [[\lambda_{ij} - \Delta\lambda_{ij}, \lambda_{ij} + \Delta\lambda_{ij}]]_{3\times3} = \begin{bmatrix} [-0.2686,\ -0.0680] & [-0.2616,\ -0.0134] & [0.5502,\ 2.0614] \\ [0.7939,\ 1.6398] & [-0.1198,\ 0.0031] & [-0.2983,\ -0.0188] \\ [-0.1103,\ 0.0132] & [0.7803,\ 1.6114] & [-0.2366,\ -0.0580] \end{bmatrix} \quad (61)$$

$$RNGA = [[\phi_{ij} - \Delta\phi_{ij}, \phi_{ij} + \Delta\phi_{ij}]]_{3\times3} = \begin{bmatrix} [-0.9732,\ -0.2153] & [-0.0178,\ 0.1330] & [0.4852,\ 2.5881] \\ [0.8796,\ 2.2665] & [-0.2164,\ -0.0114] & [-0.9162,\ -0.0021] \\ [-0.0490,\ 0.0913] & [0.5758,\ 1.5368] & [-0.1251,\ -0.0299] \end{bmatrix} \quad (62)$$

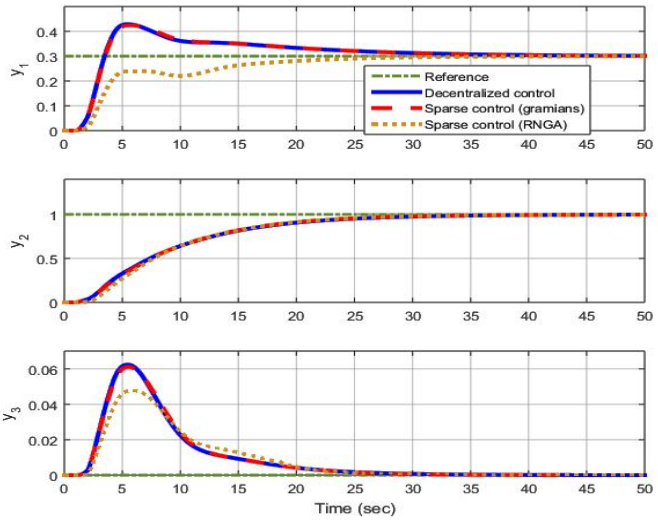

Fig. 2. Comparisons of the two measures for Example II

In (60), the varying range of the PM element for $y_1 - u_1$ has a upper bound (0.4556) much larger than the lower bound (0.2481) of that for $y_2 - u_1$, which implies it is possible that $y_1 - u_1$ instead of $y_2 - u_1$ is chosen as a paired element under the influence of the given parametric uncertainties. In contrast, (61) and (62) demonstrate that the pairing structure selected by RNGA remains the same since the λ_{ij}'s and the ϕ_{ij}'s of the paired channels ($y_1 - u_3/y_2 - u_1/y_3 - u_2$) always have dominant values in their varying ranges.

C. *Example III*

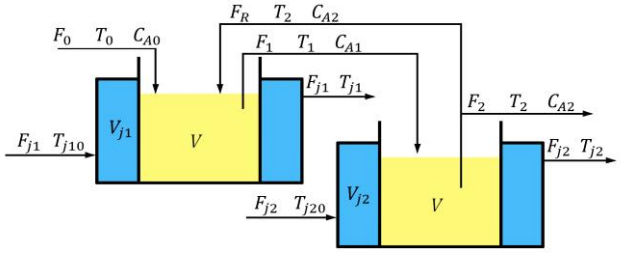

Fig. 3. Two continuous stirred-tank reactor

As a practical example, a two continuous stirred-tank reactor process [32] as shown in Fig. 3 is considered, where F_*, T_*, C_*, and V_*/V stand for flow rate, temperature, concentration, and volume, respectively. T_{j10}, T_{j20} and C_{A0} are used to regulate T_1, T_2 and C_{A2}. This process can be characterized by the following six nonlinear ordinary differential equations:

$$\begin{aligned}
\dot{x}_{11} &= (T_1^d - x_{11} + x_{31} + T_2^d)(F + F_R)/V - (x_{11} + x_{12} + T_2^d - T_{j2}^d)UA/(\rho c_p V) - (C_{A2}^d + x_{21})e^{-E/R(x_{11}+T_2^d)}\theta\delta/(\rho c_p) \\
\dot{x}_{12} &= (x_{11} + T_2^d - x_{12} - T_{j2}^d)UA/(\rho_j c_j V_j) + (u_1 + T_{j20}^d - x_{12} - T_{j2}^d)F_{j2}/V_j \\
\dot{x}_{21} &= (C_{A1}^d + x_{22})(F + F_R)/V - \left((F + F_R)/V + \theta e^{-E/R(x_{11}+T_2^d)}\right)(x_{21} + C_{A2}^d) \\
\dot{x}_{22} &= (C_{A2}^d + x_{21})F_R/V - \left((F + F_R)/V + \theta e^{-E/R(x_{31}+T_1^d)}\right)(x_{22} + C_{A1}^d) + (u_2 + C_{A0}^d)F_0/V \\
\dot{x}_{31} &= (T_2^d + x_{11})F_R/V - (x_{31} + T_1^d)(F + F_R)/V - e^{-E/R(x_{31}+T_1^d)}(x_{22} + C_{A1}^d)\theta\delta/(\rho c_p) - (x_{31} + x_{32} + T_1^d - T_{j1}^d)UA/(\rho c_p V) + T_0^d F_0/V \\
\dot{x}_{32} &= (x_{31} - x_{32} + T_1^d - T_{j1}^d)UA/(\rho_j c_j V_j) + (u_3 + T_{j10}^d - x_{32} - T_{j1}^d)F_{j1}/V_j
\end{aligned} \quad (63)$$

where $x_{11} = T_2 - T_2^d$, $x_{12} = T_{j2} - T_{j2}^d$, $x_{21} = C_{A2} - C_{A2}^d$, $x_{22} = C_{A1} - C_{A1}^d$, $x_{31} = T_1 - T_1^d$ and $x_{32} = T_{j1} - T_{j1}^d$. A three-input-three-output process can be formed where the inputs are $u_1 = T_{j20} - T_{j20}^d$, $u_2 = C_{A0} - C_{A0}^d$, and $u_3 = T_{j10} - T_{j10}^d$, and the outputs are $y_1 = x_{11}$, $y_2 = x_{21}$ and $y_3 = x_{31}$. The parameters of this process are given in Table III.

Table III. System parameters of the continuous stirred-tank reactor process

$\theta = 7.08 \times 10^{10}\ h^{-1}$	$\rho = 800.9189\ kg/m^3$	$T_0^d = 703.31$ ℃
$E = 3.1644 \times 10^7\ J/mol$	$\rho_j = 997.9450\ kg/m^3$	$T_1^d = 665.9263$ ℃
$R = 1679.2\ J/mol$℃	$c_p = 1395.3\ J/kg$℃	$T_2^d = 646.4508$ ℃
$\delta = -3.1644 \times 10^7\ J/mol$	$c_j = 1860.3\ J/kg$℃	$T_{j1}^d = 740.8$ ℃
$U = 1.3652 \times 10^6\ J/hm^2$℃	$F = 2.8317\ m^3/h$	$T_{j2}^d = 727.61$ ℃
$C_{A0}^d = 18.368\ mol/m^3$	$F_{j1} = 1.4130\ m^3/h$	$V_j = 0.1090\ m^3$
$C_{A1}^d = 12.305\ mol/m^3$	$F_{j2} = 1.4130\ m^3/h$	$V = 1.3592\ m^3$
$C_{A2}^d = 18.3679\ mol/m^3$	$F_R = 1.4158\ m^3/h$	$A = 23.226\ m^2$
$T_{j10}^d = 629.81$ ℃	$T_{j20}^d = 608.29$ ℃	$F_0 = 2.8317\ m^3/h$

The time delays are $\tau'_{ij} = 0.1s$ for all channels, and the sampling time is $T = 0.1s$. The IT2TSF model for each channel is set as $L_{ij} = 6$, $p = 2$ and $q = 0$. When collecting the input-output data samples, it can be found that u_2 has no effects on y_1 and y_3, and u_1 and u_3 cannot influence the value of y_2. Therefore, There is no need to build the models for channels $y_1 - u_2$, $y_3 - u_2$, $y_2 - u_1$ and $y_2 - u_3$. The comparisons of RMSEs between two types of fuzzy model are presented in Table IV. As can be seen, for each channel of this process, IT2TSF model achieves smaller error.

Table IV. The RMSEs of the two types of fuzzy models for (63)

	Type-1	Type-2
RMSE	$\begin{bmatrix} 0.0114 & - & 0.0584 \\ - & 0.0256 & - \\ 0.0194 & - & 0.0111 \end{bmatrix}$	$\begin{bmatrix} 0.0096 & - & 0.0406 \\ - & 0.0198 & - \\ 0.0148 & - & 0.0086 \end{bmatrix}$

We only present the first fuzzy rule of the IT2TSF model for $y_1 - u_1$ due to the limited space:

Rule 1: if $x_{11}(k)$ is $\tilde{Z}_{11}^1$, then
$\tilde{y}_1^1(k) = [0.6235, 0.8068]y_1(k-1) + [0.0708, -0.0902]y_1(k-2) + [0.1111, 0.1129]u_1(k-1)$

The center of $\tilde{Z}_{11}^{1}$ is $xc^{l} = [-0.5554 \ \ -0.3409 \ \ 3.6508]^{T}$, and $\Delta\mu^{1} = 0.0964$. Given the operating points as $x_{ij}(k_0) = [0 \ 0 \ 0]^{T}$ for $i,j = 1,2,3$, the calculated results of the two measures from IT2TSF models are:

$$TR = \begin{bmatrix} 0.0761 & 0 & 0.2794 \\ 0 & 1.0523 & 0 \\ 0.0199 & 0 & 0.0716 \end{bmatrix}, \quad PM = \begin{bmatrix} 0.0508 & 0 & 0.1864 \\ 0 & 0.7019 & 0 \\ 0.0133 & 0 & 0.0478 \end{bmatrix}$$

$$K = \begin{bmatrix} 0.3816 & 0 & 0.2553 \\ 0 & 0.9165 & 0 \\ 0.0920 & 0 & 0.3708 \end{bmatrix}, \quad E = \begin{bmatrix} 0.3334 & -0.1324 \\ -0.4181 & - \\ 0.2033 & -0.3357 \end{bmatrix}$$

$$RGA = \begin{bmatrix} 1.1990 & 0 & -0.1990 \\ 0 & 1 & 0 \\ -0.1990 & 0 & 1.1990 \end{bmatrix}, \quad \mathcal{A} = \begin{bmatrix} 1 & 0 & 0.1660 \\ 0 & 1 & 0 \\ 0.1660 & 0 & 1 \end{bmatrix}$$

$$RNGA = \begin{bmatrix} 3.2280 & 0 & -2.2280 \\ 0 & 1 & 0 \\ -2.2280 & 0 & 3.2280 \end{bmatrix}, \quad \mathcal{B} = \begin{bmatrix} 1 & 0 & 0.6902 \\ 0 & 1 & 0 \\ 0.6902 & 0 & 1 \end{bmatrix}$$

The above arrays indicate that the two measures determine different pairing structures for this process: gramians choose $y_1 - u_3/y_2 - u_2/y_3 - u_1$, and RNGA selects $y_1 - u_1/y_2 - u_2/y_3 - u_3$. In addition, gramians suggest that there is not necessary to use sparse control while RNGA using $\varepsilon_\alpha = \varepsilon_\beta = 0.1$ suggests $y_1 - u_3$ and $y_3 - u_1$ can be included to form a sparse control. Given the reference values as $rv_1 = 10, rv_2 = -2$ and $rv_3 = -8$, The control method used in Example II is applied to this process to compare the two measures. The control performance is shown in Fig. 4. As can be seen, y_1 and y_3 go divergent using the decentralized control configuration selected by gramians, while the process is stable using both decentralized and sparse control configurations selected by RNGA. This phenomenon can be explained using NI [8] introduced in the subsection *B* of Section III: the NI of the pairing structure selected by gramians is a negative number (-5.0243), which implies the process will be instable for all possible (any) values of controller parameters [8],[13]-[15],[17].

Additionally, the left part of Fig. 4 shows that the sparse control with configuration selected by RNGA achieves smaller settling time in y_1 and y_3 than the decentralized control does.

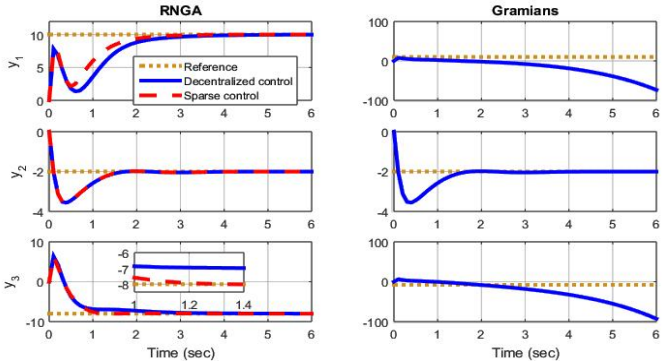

Fig. 4. Comparisons of the two measures for Example III

Suppose there are parametric variations in $b_{ij,0}$ of (16) with the varying radiuses as $\Delta b_{ij,0} = 10\% \times |b_{ij,0}|$ for $i,j = 1,2,3$, the varying ranges of the elements in PM, RGA and RNGA are:

$$PM = \left[[\psi_{ij} - \Delta\psi_{ij}, \psi_{ij} + \Delta\psi_{ij}]\right]_{3\times3} = \begin{bmatrix} [0.0315,\ 0.0700] & - & [0.1257,\ 0.2470] \\ - & [0.6182,\ 0.7856] & - \\ [0.0080,\ 0.0185] & - & [0.0296,\ 0.0659] \end{bmatrix} \quad (64)$$

$$RGA = \left[[\lambda_{ij} - \Delta\lambda_{ij}, \lambda_{ij} + \Delta\lambda_{ij}]\right]_{3\times3} = \begin{bmatrix} [1.1036,\ 1.2945] & - & [-0.3264,\ -0.0717] \\ - & [0.9204,\ 1.0796] & - \\ [-0.3264,\ -0.0717] & - & [1.1036,\ 1.2945] \end{bmatrix} \quad (65)$$

$$RNGA = \left[[\phi_{ij} - \Delta\phi_{ij}, \phi_{ij} + \Delta\phi_{ij}]\right]_{3\times3} = \begin{bmatrix} [0.3512,\ 6.1048] & - & [-5.1048,\ 0.6488] \\ - & [0.1088,\ 1.8912] & - \\ [-5.1048,\ 0.6488] & - & [0.3512,\ 6.1048] \end{bmatrix} \quad (66)$$

Equations (64)-(66) indicate that the decisions on the pairing structure made by both gramians and RNGA will not be affected by the parametric uncertainties. However, Fig. 4 shows that the pairing structure selected by gramians is not workable for this process.

The above three examples demonstrate that: **i).** IT2TSF models identified by the proposed data-driven method achieve smaller RMSEs compared to their type-1 counterparts; **ii).** Example I proves that the steady and dynamic information calculated from IT2TSF models are more accurate than that from the type-1 fuzzy models; **iii).** In the three examples, when the parameters of the models are varying in specified ranges, the pairing structures determined by RNGA remain unchanged, while in Example I and II, the decisions on pairing structure made by gramians may be affected and changed, which means RNGA is more robust to the parametric uncertainty than gramians; **iv).** The results of Example II demonstrate that the sparse control using the configuration selected by RNGA gives apparent improvement on the decentralized control, while the sparse control using the configuration selected by gramians offers the output responses negligibly different from that of decentralized control, which proves that RNGA based measure provides more reasonable sparse control configuration; **v).** In Example III, the pairing structure selected by gramians leads to instability for the closed-loop control system, while the MIMO process is stable with both decentralized and sparse control configurations selected by RNGA, and the sparse control do give an improvement compared to the decentralized control.

VI. Conclusion

This paper studied two interaction measures, one is using controllability and observability gramians, the other is using RNGA, based on IT2TSF models to evaluate the channel interactions and select control configurations for MIMO processes. A data-driven method to identify IT2TSF models was presented. Afterwards, explicit formulas to derive gramians and RNGA from the IT2TSF models were introduced, as well as the rules to choose decentralized and sparse control configuration. Next, the sensitivities of the two measures with respect to parametric variations in the IT2TSF models were investigated. Finally, the discussion to analyze and compare the two measures was given. In the case studies, three MIMO processes were used as examples to show that the proposed identification method can produce an IT2TSF model with much smaller errors than its type-1 counterpart, and RNGA based measure outperforms the gramian-based measure in terms of the control configuration selection and robustness.

REFERENCES

[1] A. Conley, M.E. Salgado, Gramian based interaction measure, *Proceedings of the 39th IEEE Conference on Decision and Control*, Sydney, Australia, 2000, pp. 5020-5022.

[2] A. Conley, M. E. Salgado, MIMO interaction measure and controller structure selection, *International Journal of Control*, 77 (2004) 367-383.

[3] H. R. Shaker, J. Stoustrup, An interaction measure for control configuration selection for multivariable bilinear systems, *Nonlinear Dynamics*, 72 (2013) 165-174.

[4] H. R. Shaker, M. Komareji, Control configuration selection for multivariable nonlinear systems, *Industrial and Engineering Chemistry Research*, 51 (2012) 8583-8587.

[5] B. Wittenmark, M. E. Salgado, Hankel-norm based interaction measure for input-output pairing, *Proceedings of the 15th IFAC World Congress*, Barcelona, Spain, 2000.

[6] M. Castano Arranz, W. Birk, On the selection of control configurations for uncertain systems using gramian-based interaction measures, *Journal of Process Control*, 47 (2016) 213-225.

[7] E.H. Bristol, On a new measure of interaction for multi-variable process control, *IEEE Transactions on Automatic Control*, 11(1966) 133-134.

[8] A. Niederlinski, A heuristic approach to the design of linear multivariable interacting subsystems, *Automatica*, 7 (1971) 691-701.

[9] P. Samuelsson, B. Halvarsson, B. Carlsson, Interaction analysis and control structure selection in a wastewater treatment plant model, *IEEE Transactions on Control Systems Technology*, 13 (2005) 955-964.

[10] M. Witcher, T.J. McAvoy, Interacting control systems: steady state and dynamic measurement of interaction, *ISA Transactions*, 16 (1977) 83-90.

[11] E.H. Bristol, Recent results on interactions in multivariable process control, in: Proceedings of the 71st Annual AIChE Meeting, Houston, TX, USA, 1979.

[12] T. McAvoy, Y. Arkun, R. Chen, D. Robinson, P.D. Schnelle, A new approach to defining a dynamic relative gain, *Control Engineering Practice*, 11 (2003) 907-914.

[13] Q. Xiong, W.J. Cai, M.J. He, A practical loop pairing criterion for multivariable processes, *Journal of Process Control*, 15 (2005) 741-747.

[14] M.J. He, W.J. Cai, W. Ni, L.H. Xie, RNGA based control system configuration for multivariable processes, *Journal of Process Control*, 19 (2009) 1036-1042.

[15] Y.L. Shen, W.J. Cai, S.Y. Li, Multivariable process control: decentralized, decoupling, or sparse? *Industrial & Engineering Chemistry Research*, 49 (2010) 761-771.

[16] C.Y. Xu, Y.C. Shin, Interaction analysis for MIMO nonlinear systems based on a fuzzy basis function network model, *Fuzzy Sets and Systems*, 158 (2007) 2013-2025.

[17] Q.F. Liao, W.J. Cai, S.Y. Li, Y.Y. Wang, Interaction analysis and loop pairing for MIMO processes described by T-S fuzzy models, *Fuzzy Sets and Systems*, 207 (2012) 64-76.

[18] L.X. Wang, J.M. Mendel, Fuzzy basis functions, universal approximation, and orthogonal least-squares learning, *IEEE Transactions on Neural Networks*, 3 (1992) 807-814.

[19] Q.L. Liang, J.M. Mendel, An introduction to type-2 TSK fuzzy logic systems, *IEEE International Fuzzy Systems. Conference Proceedings*, Seoul, South Korea, 1999, pp. 1534-1539

[20] N.N. Karnik, J.M. Mendel, Q.L Liang, Type-2 fuzzy logic systems, *IEEE Transactions on Fuzzy Systems*, 7 (1999) 643-658

[21] J.M. Mendel, On KM algorithms for solving Type-2 fuzzy set problems, *IEEE Transactions on Fuzzy Systems*, 21 (2013) 426-446

[22] Q.F. Liao, D. Sun, W.J. Cai, S.Y. Li, Y.Y. Wang, Type-1 and Type-2 effective Takagi-Sugeno fuzzy models for decentralized control of multi-input-multi-output processes, *Journal of Process Control* 52 (2017) 26-44.

[23] D. Sun, Q. Liao, H. Ren, Type-2 fuzzy modeling and control for bilateral teleoperation system with dynamic uncertainties and time-varying delays, *IEEE Transactions on Industrial Electronics*, 99 (2017) 1-13.

[24] D. E. Gustafson, W. C. Kessel, Fuzzy clustering with a fuzzy covariance matrix, *IEEE Conference on Decision and Control including the 17th Symposium on Adaptive Processes*, San Diego, USA, 1978, pp. 761-766.

[25] J.M. Mendel, Computing Derivatives in Interval Type-2 Fuzzy Logic Systems, *IEEE Transactions on Fuzzy Systems*, 12 (2004) 84-98.

[26] S. Bittanti, P. Bolzern, and M. Campi, Recursive least-squares identification algorithms with incomplete excitation: convergence analysis and application to adaptive control, *IEEE Transactions on Automatic Control*, 35 (1990) 1371-1373

[27] L. Ljung, System Identification: Theory for the User, second ed., Prentice-Hall Inc., Englewood Cliffs, NJ, 1999.

[28] Q. Xiong, W.J. Cai, M.J. He, Equivalent transfer function method for PI/PID controller design of MIMO processes, *Journal of Process Control*, 17 (2007) 665-673.

[29] D. Chen, D. E. Seborg, Relative Gain Array Analysis for Uncertain Process Models, *AIChE Journal*, 48 (2002) 302-310.

[30] H.P. Huang, J.C. Jeng, C.H. Chiang, W. Pan, A direct method for multi-loop PI/PID controller design, *Journal of Process Control* 13(2003) 769-786.

[31] Q. Xiong, W.J. Cai, Effective transfer function method for decentralized control system design of multi-input multi-output processes, *Journal of Process Control* 16(2006) 773-784.

[32] B. Chen, X.P. Liu, K.F. Liu, C. Lin, Adaptive fuzzy tracking control of nonlinear MIMO systems with time-varying delays, *Fuzzy Sets and Systems*, 217 (2013) 1-21.